MPM with frictional contact for application to soft particulate materials

Saeid Nezamabadi, Thanh Hai Nguyen, Jean-Yves Delenne, Julien Averseng, Xavier Frank, Farhang Radjai

▶ **To cite this version:**

HAL Id: hal-01494427
https://hal.science/hal-01494427

Submitted on 23 Mar 2017

1st International Conference on the Material Point Method, MPM 2017

MPM with frictional contact for application to soft particulate materials

Saeid Nezamabadi[a,*], Thanh H. Nguyen[a,c], Jean-Yves Delenne[b], Julien Averseng[a], Xavier Frank[b], Farhang Radjai[a,d]

[a]*Laboratoire de Mécanique et Génie Civil (LMGC), Université de Montpellier, CNRS, Montpellier, France*
[b]*Ingénierie des Agro-polymères et Technologies Émergentes (IATE), UMR1208, INRA, Université de Montpellier, Cirad, SupAgro, Montpellier, France*
[c]*Water Resources Engineering Department, Da Nang University of Technology, Da Nang University, 54 Nguyen Luong Bang St, LienChieu Dist, Da Nang, Vietnam*
[d]*<MSE>[2] , UMI 3466 CNRS-MIT, CEE, Massachusetts Institute of Technology (MIT), 77 Massachusetts Avenue, Cambridge CA 02139, USA*

Abstract

Soft particle materials are composed of discrete particles that can undergo large deformations without rupture. Most food products, many powders, colloidal pastes, vesicles and biological cells are soft particle systems. In order to model such materials, we present an efficient numerical approach combining an implicit formulation of the Material Point Method (MPM) and Contact Dynamics (CD) method. The MPM deals with bulk variables of an individual particle by discretizing it as a collection of material points, whereas the CD allows for the treatment of frictional contacts between particles. This model is applied for the simulation of the uni-axial compression of 2D soft-particle packings. The compaction is a nonlinear process in which new contacts are formed between particles and the contact areas increase. The change of particle shapes allows these materials to reach high packing fraction. We find that the contact specific surface, the orientation anisotropy and the aspect ratio of particles increase as a function of the packing fraction but at different rates. We also evidence the effect of friction, which favors strong stress chains and thus the elongation of particles, leading to larger values of the orientation anisotropy and the aspect ratio at a given level of packing fraction as compared to a frictionless particle packing.

1. Introduction

Soft particles are the main component of many natural and industrials materials like colloidal pastes, microgels, suspensions, etc. In these materials, there is a disordered discrete network of soft particles which governs their behaviors by a combination of particle rearrangements and particle shape change. So, the properties of soft particle materials depend on both theirs discrete natures (contact interactions, rearrangements...) and their particle continuum

---

* Corresponding author.
E-mail address: saeid.nezamabadi@umontpellier.fr

behaviors (deformability, compressibility...). Indeed, these particles can undergo large deformation without rupture. All of these features allow these materials to achieve high packing fractions beyond Random Close Packing (RCP) state. Because of these complexities of soft particle systems, many aspects of their behaviors and properties under compression and shear should be until explored.

Particular materials are mainly simulated using numerical strategies based on Discrete Element Methods (DEM). In the DEM, these materials are modeled as a collection of undeformable particles and the elastic deformations may be assumed at the contact points. The most common discrete methods based on hard particles are Molecular Dynamics (MD) [1] and Contact Dynamics (CD) [2,3]. Although the DEM techniques are known as mature and efficient approaches to model and analyze particular materials, they are intrinsically unable to account for realistic constitutive models of individual particles and large particle deformations. So, in order to deal with both continuum and discrete behaviors of soft particle materials, it is necessary to introduce the internal degrees of freedom for each individual particule as well as to treat contact interaction between different particles.

A promising numerical procedure has been developed to investigate a packing of soft particles in our previous papers [4,5]. This approach combines two numerical tools: it uses first an implicit formulation of Material Point Method (MPM) [6] to take into account the constitutive continuum behaviors of particles. In this approach, each particle is discretized by a collection of material points. The information carried by the material points is projected onto a background mesh, where equations of motion are solved. The mesh solution is then used to update the material points. The second tool which is related to the contact treatment, is based on the Contact Dynamics. The CD method is a general approach for the treatment of frictional contacts without regularization. It was pioneered by a mathematical formulation of non-smooth mechanics by Moreau [7] and then extensively used for the simulation of granular materials with rigid grains [8,9]. This method is based on an implicit time-stepping scheme and formulated in terms of grain velocities, which may undergo jumps as a result of collisions and non-smooth feature of the Coulomb friction law. Since we use an implicit MPM scheme, the CD method is a natural choice for the treatment of contact points. The implicit MPM-CD formulation was implemented in a manner that the contact variables can be computed simultaneously with bulk variables. In this paper, we apply this MPM algorithm to analyze the compaction of a packing of soft particles. We investigate the respective roles of rearrangements, particle volume change and particle shape change to compaction by analyzing different rheological parameters (packing fraction and, contact specific surface, orientation anisotropy and aspect ratio of particles).

2. Material point method (MPM)

Let us consider a continuum body occupying a domain Ω in $\mathbb{R}^D$, D being the domain dimension. In the context of the infinitesimal strain theory, its conservations of mass and of linear momentum can be described by the following relations:

$$\frac{\partial \rho(\mathbf{x}, t)}{\partial t} + \boldsymbol{\nabla} \cdot (\rho(\mathbf{x}, t)\, \mathbf{v}(\mathbf{x}, t)) = 0 \quad \text{in } \Omega, \tag{1}$$

$$\boldsymbol{\nabla} \cdot \boldsymbol{\sigma}(\mathbf{x}, t) + \mathbf{b}(\mathbf{x}, t) = \rho(\mathbf{x}, t)\, \mathbf{a}(\mathbf{x}, t) \quad \text{in } \Omega, \tag{2}$$

where $\rho(\mathbf{x}, t)$ is the material density, $\boldsymbol{\sigma}(\mathbf{x}, t)$ denotes the Cauchy stress tensor, $\mathbf{b}(\mathbf{x}, t)$ represents the body force and, $\mathbf{v}(\mathbf{x}, t)$ and $\mathbf{a}(\mathbf{x}, t)$ are the velocity and the acceleration, respectively, at position $\mathbf{x}$ and time t. A constitutive relationship should supplement the continuity equation (1) and momentum equation (2). We assume here a linear, homogeneous, isotropic and elastic relationship:

$$\boldsymbol{\sigma}(\mathbf{x}, t) = \mathbb{C} : \boldsymbol{\epsilon}(\mathbf{x}, t), \tag{3}$$

where $\mathbb{C}$ refers to fourth-order elastic tensor and $\boldsymbol{\epsilon}$ denotes the strain tensor ($\boldsymbol{\epsilon} = \frac{1}{2}(\boldsymbol{\nabla}\mathbf{u} +^t \boldsymbol{\nabla}\mathbf{u})$; $\mathbf{u}$ being the displacement field). Note that, in this formulation, any other material behavior (including inelastic behaviors) may be implemented.

In the MPM, the continuum body is divided into N_p material points with constant masses. This last assumption allows satisfying automatically the mass conservation relation (1). The material points represent the integration points

to compute the integrals in the context of the finite element method. However, the MPM discretizes these integrals through a Dirac delta function. For instance, the density can be discretized for an element in the following form:

$$\rho(\mathbf{x}, t) = \sum_{p=1}^{N_p} \rho_p \, \delta(\mathbf{x} - \mathbf{X}_p(t)) , \tag{4}$$

where ρ_p ($\rho_p = m_p/V_p$ with material point mass m_p and volume V_p) is material point density, $\mathbf{X}_p(t)$ refers to position of material point and δ denotes the Dirac delta function.

By supposing contact interactions between bodies, the discretized form of the momentum equation can be written as:

$$\mathbf{M} \, \mathbf{a}_{\text{node}}(t) = \mathbf{F}^{\text{int}}(t) + \mathbf{F}^{\text{ext}}(t) + \mathbf{F}^{\text{C}}(t) , \tag{5}$$

where $\mathbf{a}_{\text{node}}$ is the nodal acceleration, $\mathbf{F}^{\text{C}}$ denotes the contact force (see below), $\mathbf{F}^{\text{ext}}$ represents the external applied force, and

$$\mathbf{M} = \sum_{e=1}^{N_e} \sum_{p=1}^{N_p} m_p \, \mathbf{N}_p , \qquad \mathbf{F}^{\text{int}} = - \sum_{e=1}^{N_e} \sum_{p=1}^{N_p} \mathbf{G}_p \, \sigma_p \, V_p . \tag{6}$$

In the above equations, $\mathbf{M}$ is the lumped mass matrix and $\mathbf{F}^{\text{int}}$ gives the internal force vector resulting from the stress divergence. $\mathbf{N}_p$ denotes interpolation matrix or shape function matrix and $\mathbf{G}_p$ represents the gradient of the shape function $\mathbf{N}_p$ at $\mathbf{X_p}$.

Nodal velocities $\mathbf{v}_{\text{node}}$ can be computed from the material point velocities $\mathbf{v}_p$ using a weighted least-squares procedure:

$$\mathbf{P}_{\text{node}} = \mathbf{M} \, \mathbf{v}_{\text{node}} = \sum_{e=1}^{N_e} \sum_{p=1}^{N_p} m_p \, \mathbf{N}_p \, \mathbf{v}_p , \tag{7}$$

where $\mathbf{P}_{\text{node}}$ is the nodal momentum. Applying this approach is justified by the fact that there are generally more material points than grid nodes.

A MPM implicit approach is implemented to solve the problem (5) [4]. The nodal solutions are projected onto the material points, allowing for updating the information carried by these points.

Furthermore, since we aim to treat the packings of deformable particles, the contact interactions are considered in the movement equations, $\mathbf{F}^{\text{C}}$. These contact forces between particles need to be calculated by means of a contact algorithm accounting for the condition of non-interpenetration of matter as well as the Coulomb friction law. So, our implicit MPM scheme is combined with the Contact Dynamic (CD) method which is also an implicit procedure. For this reason, the CD method can be considered as a natural choice for the treatment of contact points. In the MPM, a multi-mesh mapping can be used to implement contact laws such as the friction Coulomb law or adhesion laws at the contact points [10,11]. In such models the contact variables are computed simultaneously with bulk stresses and strains.

Let us consider two deformable particles(α and β); see Fig. 1a. In the context of multi-mesh algorithm, each particle maps in its proper background mesh. A contact point at the interface between the two particles may be treated by introducing a common background mesh with the same type of grids for the transfer of nodal quantities from proper meshes to the common mesh. The contact points between the particles α and β are treated at the neighboring nodes belonging to the common background mesh. Their nodal values involve contributions from the two particles. At a potential contact node i, a normal unit vector $\mathbf{n}_i$, oriented from particle β to particle α, and a tangential unit vector $\mathbf{t}_i$ are defined [12]. As long as the normal velocity v_n ($v_n = (\mathbf{v}_i^\alpha - \mathbf{v}_i^\beta) \cdot \mathbf{n}_i$) remains positive, the normal force f_n is identically zero. But when $v_n = 0$, a non-negative (repulsive) normal force f_n is mobilized at the contact node. These conditions define the velocity-Signorini complementary condition as shown in Fig. 1b [13,14]. On the other hand, by combining the equations of motion $\mathbf{P}_{\text{node}}^\alpha = \mathbf{M}^\alpha \, \mathbf{v}_{\text{node}}^\alpha$ and $\mathbf{P}_{\text{node}}^\beta = \mathbf{M}^\beta \, \mathbf{v}_{\text{node}}^\beta$ at the common node, we get a linear relation $f_n = M_n v_n + k_n$, where M_n is the reduced mass and k_n is an offset force which depends on the internal and external forces as well as the relative velocity at the beginning of a time step and other contact forces. The normal
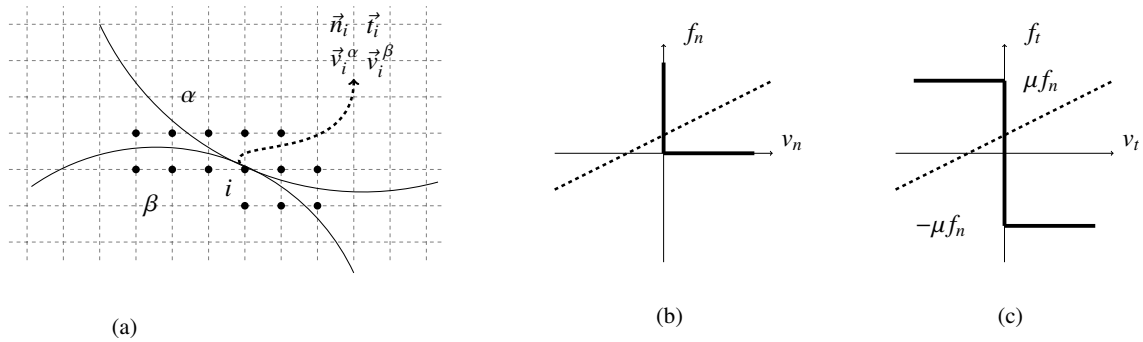
Fig. 1: (a) Multi-mesh contact algorithm scheme in MPM. The solid points represent the potentiel contact nodes (see text); (b-c) Contact conditions: (b) Signorini graph relating the normal relative velocity v_n and normal force f_n; (c) Coulomb graph relating the sliding velocity v_t and friction force f_t; μ is the coefficient of friction. The dashed lines represent linear relations extracted from the equations of dynamics.

force at all contact nodes are obtained through an iterative process by intersecting the above linear relation with the Signorini graph, as shown in Fig. 1b.

In a similar vein, the Coulomb law of dry friction is a complementarity relation between the friction force f_t and the tangential velocity v_t ($v_t = (\mathbf{v}_i^\alpha - \mathbf{v}_i^\beta) \cdot \mathbf{t}_i$) at the contact node; see Fig. 1c. Like the Signorini graph, the Coulomb law is a complementarity relation in the sense that it can not be reduced to a single-valued function. The equations of motion at the common node yield a linear relation $f_t = M_t v_t + k_t$, which is intersected with the Coulomb graph to calculated the friction force f_t simultaneously at all contact nodes in the same iterative process used to calculate the normal forces. The convergence to the solution both for contact forces and internal stresses is smooth, and a high precision may be achieved through the convergence criterion. The details of our MPM procedure are given in a previous paper [4].

3. Uni-axial compression of a soft particle system

In this section, we use the MPM-CD coupled algorithm to analyze the compaction of a packing of soft particles. It is composed of 300 soft disks confined inside a rectangular box of width L in which only the top wall is mobile and moves downwards at constant velocity of 2 m/s. The box walls are also modeled using the MPM. The initial configuration is prepared by means of CD simulations. A small size polydispersity is introduced in order to avoid long-range ordering; the particles' radii vary from 0.7 mm to 1.2 mm. The gravitational acceleration is set to be zero in order to avoid stress gradients. We consider two cases below: 1) without friction and 2) with a high coefficient of friction $\mu = 0.5$ between the particles. There is no friction between the particles and the walls. This allows for higher degree of homogeneity in stress transmission. The particles are supposed to behave elastically with Young's modulus of $E = 10$ MPa and Poisson's ratio of $\nu = 0.45$. We used this value for Poisson's ratio in order to favor particle shape change compared to particle volume change. The particle density is set to $\rho = 990$ kg/m^3. A time step of $\delta t = 0.5$ μs is considered for these simulations.

Three effects contribute to the increase of packing fraction: (i) particle rearrangements, (ii) elastic volume change of the particles and (iii) particle shape change. Since we are interested here in the mechanisms by which the particles exceed the RCP limit, the evolution of the packing fraction is analyzed in terms of the mean values of contact specific surface S, orientation anisotropy A_m and aspect ratio α of the particles; see Fig. 2. These quantities are defined as follows:

$$S = \frac{\sum_{g=1}^{N_g} S_g^C}{\sum_{g=1}^{N_g} \pi D_g}, \qquad A_m = 2(G_1 - G_2), \qquad \alpha = \frac{1}{N_g} \sum_{g=1}^{N_g} \frac{l_{1_g}}{l_{2_g}}, \qquad (8)$$

where N_g is the total number of the particles, D_g, S_g^C and V_g denote the diameter, contact surface and volume of the
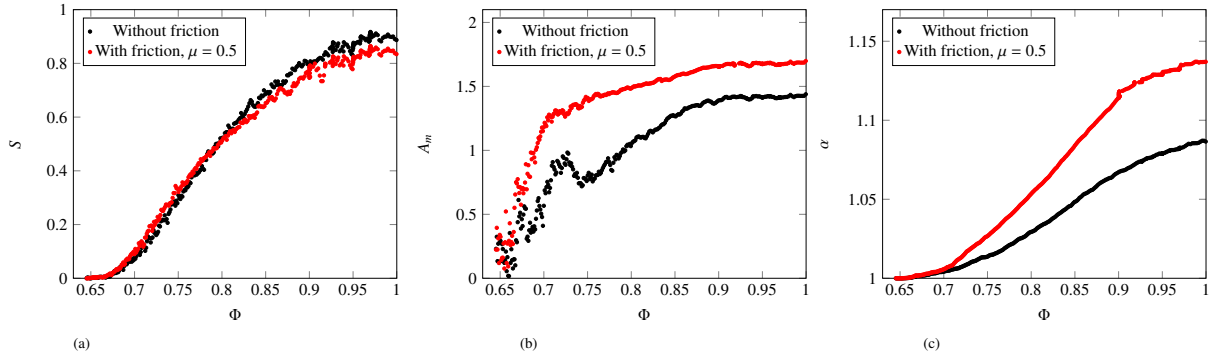
Fig. 2: Evolutions of mean contact specific surface S, mean orientation anisotropy A_m and mean aspect ratio α as a function of packing fraction Φ.
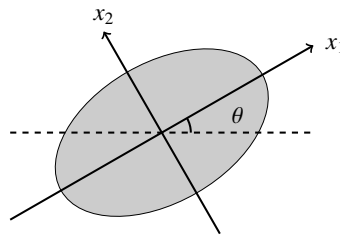

Fig. 3: Schematic of a deformed particle in which the particle orientation θ and its principal axes x_1 and x_2 are represented.

particle g, respectively, and l_{1_g} and l_{2_g} represent its longest and shortest dimensions along its principal axes x_1 and x_2; Fig. 3. Furthermore, G_1 and G_2 $(G_1 > G_2)$ are the eigenvalues of the fabric tensor $\mathbf{F}$ defined by:

$$\mathbf{G} = \begin{bmatrix} \dfrac{1}{N_g} \sum_{g=1}^{N_g} \cos^2(\theta_g) & \dfrac{1}{N_g} \sum_{g=1}^{N_g} \cos(\theta_g)\sin(\theta_g) \\ \dfrac{1}{N_g} \sum_{g=1}^{N_g} \cos(\theta_g)\sin(\theta_g) & \dfrac{1}{N_g} \sum_{g=1}^{N_g} \sin^2(\theta_g) \end{bmatrix}, \tag{9}$$

with the particle orientation θ as illustrated in Fig. 3.

As observed in Fig. 2, the three variables S, A_m and α increase as a function of the packing fraction Φ at different rates. Hence, three regimes may be distinguished. In the first regime ($\Phi < 0.72$), the particle configuration evolves as a result of global rearrangements. The evolution of S, A_m and α is due to the elongation of nearly all particles in the second regime ($0.72 < \Phi < 0.9$). Here, although the contact specific surface S varies approximately at a same rate for the frictionless and frictional cases, the particle aspect ratio α grows at a higher rate for frictional case in comparison to the frictionless one. Moreover, the value of the particle orientation anisotropy A_m for the frictional case is larger than the frictionless one while A_m evaluates at slower rate for frictional particles. Indeed, in this regime, the friction between particles allows for stronger and more linear stress chains as compared to frictionless particles, and thus it leads to more elongated particles in the frictional case, as you can see in Fig. 4 [4]. This figure shows some snapshots of the compaction test by MPM simulation. The particle shapes evolve from circular to nearly polygonal as shown in Fig.4, and the void space is filled by the particles. Furthermore, for frictionless particles, the variation of A_m decreases for packing fractions ranging from 0.72 to 0.75. It can be explained by particle rearrangements due to deformation-induced sliding whereas frictional particles cannot move freely due to friction. In the third regime ($\Phi < 0.9$), the particles can no more slide and move so that S, A_m and α vary at a slower rate than in the second regime.

(a) Φ = 0.65; Initial state   (b) Φ = 0.9; Frictionless particles   (c) Φ = 0.9; Frictional particles
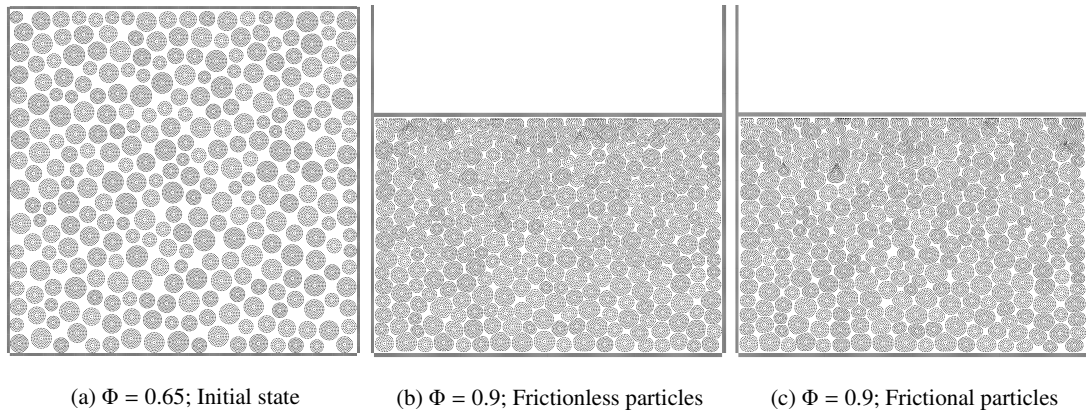
Fig. 4: The snapshots of the compaction of a packing of soft particles. Filled Circles are material points in the MPM.

4. Conclusion

This paper was concerned with the mechanical modeling of soft-particle materials by interfacing the Material Point Method, for dealing with the bulk behavior of particles, with the Contact Dynamics method for the treatment of frictional contacts. From simulations of the uniaxial compaction of an assembly of elastic particles, we analyzed the relationship between particle shape change and the evolution of the packing fraction. In particular, it was shown that the friction increases the stress ratio of the particles and hence leads to higher particle shape change. As a result, the aspect ratio and orientational anisotropy of frictional particles are above that of frictionless particles whereas their contact specific surface remains approximately constant.

Acknowledgment

References

[1] F. Radjai, F. Dubois (Eds.), Discrete-element Modeling of Granular Materials, Iste-Wiley, London, 2011.
[2] J. Moreau, Some numerical methods in multibody dynamics : application to granular, European J. Mech. A Solids 13 (1994) 93–114.
[3] F. Radjai, V. Richefeu, Contact dynamics as a nonsmooth discrete element method, Mechanics of Materials 41 (2009) 715–728.
[4] S. Nezamabadi, F. Radjai, J. Averseng, J.-Y. Delenne, Implicit frictional-contact model for soft particle systems, Journal of the Mechanics and Physics of Solids 83 (2015) 72–87.
[5] S. Nezamabadi, T. Nguyen, J.-Y. Delenne, F. Radjai, Modeling soft granular materials, Granular Matter Accepted (2016).
[6] J. Guilkey, J. Weiss, Implicit time integration for the material point method: quantitative and algorithmic comparisons with the finite element method, International Journal for Numerical Methods in Engineering 57 (2003) 1323–1338.
[7] J.-J. Moreau, Unilateral contact and dry friction in finite freedom dynamics, volume 302 of *International Centre for Mechanical Sciences, Courses and Lectures*, Springer, Vienna, 1988.
[8] F. Radjai, M. Jean, J.-J. Moreau, S. Roux, Force distributions in dense two-dimensional granular systems, Physical Review Letters 77 (1996) 274–277.
[9] T. Unger, L. Brendel, D. E. Wolf, J. Kertsz, Elastic behavior in contact dynamics of rigid particles., Phys Rev E Stat Nonlin Soft Matter Phys 65 (2002) 061305.
[10] S. Bardenhagen, J. Guilkey, K. Roessig, J. Brackbill, W. Witzel, J. Foster, An improved contact algorithm for the material point method and application to stress propagation in granular material, Computer Modelling in Engineering and Sciences 22 (2001) 509–522.
[11] X. Pan, A. Xu, G. Zhang, P. Zhang, J. Zhu, S. Ma, X. Zhang, Three-dimensional multi-mesh material point method for solving collision problems, Communications in Theoretical Physics 49 (2008) 1129–1138.

[12] P. Huang, X. Zhang, S. Ma, X. Huang, Contact algorithms for the material point method in impact and penetration simulation, International Journal for Numerical Methods in Engineering 85 (2011) 498–517.

[13] M. Jean, Frictional contact in rigid or deformable bodies: numerical simulation of geomaterials, Elsevier Science Publisher, Amsterdam, 1995, pp. 463–486.

[14] B. Brogliato, Nonsmooth mechanics, Springer, London, 1999.